

Chapter 2

METHODS FOR QUANTITATIVE CHARACTERIZATION OF LANDSCAPE PATTERN

1. Single-resolution Measurements

Once a land cover map is in hand, the simplest characterization of a landscape is the marginal (non-spatial) land cover distribution which is estimated from the readily available land cover proportions. Although the marginal distribution may be tightly linked to spatial pattern (Gustafson and Parker, 1992), two very different landscapes can still yield the same marginal distribution; therefore, additional measurements of specific aspects of spatial pattern are needed to properly characterize landscapes.

Many measurements of landscape pattern are available and most have been conveniently coded and made available as public domain software under the title of “FRAGSTATS” (McGarigal and Marks, 1995; www.umass.edu/landeco/research/fragstats/fragstats.html, accessed January, 2006). Many of these measurements are highly inter-correlated (Riitters, *et al.*, 1995; Hargis, Bissonette and David, 1998); therefore, one typically wants to select an appropriate subset.

The initial set of landscape variables that are applied in later chapters for the Pennsylvania watersheds are listed in Table 2.1. These measurements are based on eight different land cover types, as discussed in Section 4.1 of Chapter 1. Table 2.1 also includes land cover proportion summaries that were included with the pattern variables for subsequent analytical purposes. The land covers were summarized as follows: All forest cover types (conifer, mixed and deciduous) were summed to yield the proportion of “Total Forest” cover, and annual herbaceous and perennial herbaceous land was summed to yield “Total Herbaceous” cover.

Terrestrial unvegetated land was also included to capture much of the urban land.

Table 2.1. Landscape variables measured for Pennsylvania watersheds.

<i>Variable Description</i>	<i>Code</i>
Patch Density	PD
Mean Patch Size	MPS
Patch Size Coefficient of Variation	PSCV
Edge Density	ED
Landscape Shape Index	LSI
Area-Weighted Mean Shape Index	AWMSI
Double-Log Fractal Dimension	DLFD
Area-Weighted Mean Patch Fractal Dimension	AWMPFD
Shannon Evenness Index	SHEI
Interspersion and Juxtaposition Index	IJI
Contagion [†]	CONTAG
Total Forest Cover	TOT.FOREST
Total Herbaceous Cover	TOT.HERB
Terrestrial Unvegetated	TU

note that diagonally adjacent pixels were included when determining patches

[†] pixel order preserved when measuring contagion

The spatial pattern measurements in Table 2.1 represent diverse aspects of pattern such as responses to average patch size, patch size distribution and patch shape complexity. *Patch density* and *edge density* are the number of distinct patches or edges, respectively, divided by the total landscape area. The *mean patch size* is the total landscape area divided by the number of distinct patches. The *patch size coefficient of variation* is the patch size standard deviation divided by the mean patch size.

The *landscape shape index* is the sum of the landscape boundary and all edge segments within the landscape boundary divided by the square root of the total landscape area, adjusted by a constant for a square standard. To formulate, let E equal the total length of edge, including the entire landscape boundary and background edge segments, regardless of whether or not they represent true edge, and let A equal the total landscape area. Then, for a raster land cover map,

$$LSI = \frac{0.25E}{\sqrt{A}} .$$

As the LSI increases above 1, the landscape shape becomes more irregular or the length of edge within the landscape increases or both. The *area-weighted mean shape index* is the sum, across all patches, of each

patch perimeter divided by the square root of patch area, adjusted by a constant for a square standard, multiplied by the patch area and divided by the total landscape area. To formulate, for $i = 1, \dots, k$ patch types (land cover categories) and $j = 1, \dots, n_i$ patches within type i , let p_{ij} and a_{ij} equal the perimeter and area, respectively, for the j^{th} patch of the i^{th} type. Then,

$$AWMSI = \sum_{i=1}^k \sum_{j=1}^{n_i} \left(\frac{0.25p_{ij}}{\sqrt{a_{ij}}} \right) \left(\frac{a_{ij}}{A} \right).$$

The AWMSI provides an average shape index of patches, weighted by patch area so that large patches are weighted higher than smaller ones. As with the LSI, the patch shapes become more irregular as AWMSI increases above 1.

The perimeter/area scaling exponent, called the double-log fractal dimension (DLFD) by FRAGSTATS, equals 2 divided by the slope of the regression line obtained by regressing the logarithm of patch area against the logarithm of patch perimeter. With limits of 1 and 2, the DLFD reflects more Euclidean shaped patches as DLFD approaches 1 and reflects patches with more convoluted, plane filling perimeters as DLFD approaches 2. The *area-weighted mean patch fractal dimension* equals the sum, across all patches, of 2 times the logarithm of patch perimeter divided by the logarithm of patch area, multiplied by the patch area and divided by the total landscape area. This is expressed as

$$AWMPFD = \sum_{i=1}^k \sum_{j=1}^{n_i} \left(\frac{2\log(0.25p_{ij})}{\log a_{ij}} \right) \left(\frac{a_{ij}}{A} \right).$$

Shannon evenness was chosen to characterize the marginal land cover distribution, and is simply the Shannon entropy of the land cover proportions divided by the maximum attainable entropy. Therefore, for $i = 1, \dots, k$ land cover types and P_i equals the proportion of data pixels in the landscape that are categorized as type i ,

$$SHEI = \frac{-\sum_{i=1}^k P_i \log P_i}{\log(k)},$$

and as SHEI approaches 0 from above, the landscape is increasingly dominated by particular land cover types, whereas as SHEI approaches 1 from below, the distribution of land cover types becomes increasingly more even.

The *interspersion and juxtaposition* and *Shannon contagion* indices respond to both the composition and configuration of landscape pattern.

For contagion, consider a cell adjacency matrix where each element A_{ij} is the number of pixels in the raster map of category i that are adjacent to category j ; then let $v_{ij} = \frac{A_{ij}}{\sum_{i=1}^k \sum_{j=i}^k A_{ij}}$. Shannon evenness of the adjacency matrix can then be obtained, and it's compliment is taken as a measure of contagion as

$$\text{SHCO} = 1 + \frac{\sum_{i=1}^k \sum_{j=i}^k v_{ij} \log(v_{ij})}{2\log(k)}.$$

The interspersion and juxtaposition index is similar to Shannon contagion, except that it quantifies the unevenness of the *patch* adjacency matrix, as opposed to the cell adjacency matrix. For k land cover types, let e_{ij} equal the total length of edge in the landscape between land cover types i and j , and let E equal the total length of edge in the landscape. Interspersion and juxtaposition is then measured by

$$\text{IJI} = -\frac{\sum_{i=1}^k \sum_{j=i+1}^k \frac{e_{ij}}{E} \log(\frac{e_{ij}}{E})}{\log(\frac{1}{2}k(k-1))}.$$

2. The Conditional Entropy Profile

Johnson, Tempelman and Patil (1995) introduce conditional entropy as a basis for quantifying spatial fragmentation patterns as one moves from coarser- to finer-resolution categorical raster maps of a landscape. We now present the concept of conditional entropy, followed by a computational approach in the case of multiple raster map resolutions that are obtained by scaling up from a floor resolution by a random filter.

Consider a raster map whose pixels are each assigned one of k distinct land cover categories that are in turn represented by distinct colors. Now consider a map of the same extent that consists of four times as many pixels such that they are hierarchically nested within the larger pixels of the first map. This sequence of increasing resolution may continue so that for an arbitrary n^{th} scale (resolution), each pixel can be sub-divided into four “child” pixels at the $n + 1$ scale, and is itself a child pixel of a “parent” pixel from the $n - 1$ scale. This process is diagrammed in Figure 2.1.

Letting the most coarse scale map be level 0, and the finest scale (floor resolution) be level L , we thus have a sequence M_0, \dots, M_L of maps with increasingly finer resolution. For the n^{th} resolution, let $\hat{P}_i^{[n]}$ equal the proportion of pixels from the n^{th} scaled map that are labeled as category i for $i = 1, \dots, k$, where the “hat” symbolizes a quantity that is calculated from data. For each set of four child pixels at scale $n + 1$ that are nested within a single parent pixel, let \mathbf{s} be a vector containing

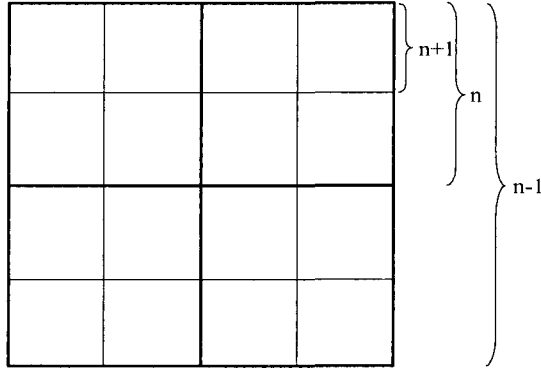


Figure 2.1. Hierarchical nesting of pixels.

a unique ordering of four out of k categories for $\mathbf{s} = 1, \dots, k^4$, where the ordering is according to the pixel sequence: NW corner, NE corner, SW corner, SE corner.

Let $\hat{P}_{\mathbf{s}}^{[n+1]}$ equal the proportion of child “4-tuples” that yield the vector \mathbf{s} at scale $n + 1$. Now define $\hat{P}_{i\mathbf{s}}^{[n,n+1]}$ as the proportion of “4-tuples” at scale $n + 1$ that are of vector \mathbf{s} , given a parent pixel of category i , and define $\hat{P}_{si}^{[n+1,n]}$ as the proportion of parent pixels in category i , given that a child 4-tuple is of vector \mathbf{s} .

For a particular scale n , the marginal entropy of the parent pixels from the n scaled map is computed as

$$\hat{H}^{[n]} = - \sum_{i=1}^k \hat{P}_i^{[n]} \log \hat{P}_i^{[n]}, \quad (2.1)$$

the marginal entropy of the child 4-tuples from the $n + 1$ scaled map is computed as

$$\hat{H}^{[n+1]} = - \sum_{\mathbf{s}=1}^{k^4} \hat{P}_{\mathbf{s}}^{[n+1]} \log \hat{P}_{\mathbf{s}}^{[n+1]}, \quad (2.2)$$

the conditional entropy of the parent scale categories, given the child scale 4-tuples is computed as

$$\hat{H}^{[n+1,n]} = - \sum_{\mathbf{s}=1}^{k^4} \hat{P}_{\mathbf{s}}^{[n+1]} \sum_{i=1}^k \hat{P}_{si}^{[n+1,n]} \log \hat{P}_{si}^{[n+1,n]}, \quad (2.3)$$

and the conditional entropy of the child scale 4-tuples given the parent scale categories is computed as

$$\hat{H}^{[n,n+1]} = - \sum_{i=1}^k \hat{P}_i^{[n]} \sum_{s=1}^{k^4} \hat{P}_{is}^{[n,n+1]} \log \hat{P}_{is}^{[n,n+1]}, \quad (2.4)$$

where $x \log(x)$ equals 0 when $x = 0$.

The objective is to obtain this last expression $\hat{H}^{[n,n+1]}$, although it is difficult to compute directly. However, since the total entropy of cross-classified factors can be decomposed into among and within sources (i.e. Patil and Taillie, 1982; Pileou, 1975; Colwell, 1974), the entropy components just discussed are related as

$$\hat{H}^{[n]} + \hat{H}^{[n,n+1]} = \hat{H}^{[n+1]} + \hat{H}^{[n+1,n]}. \quad (2.5)$$

Therefore, if the other three entropy components are obtained, as will be discussed shortly, then $\hat{H}^{[n,n+1]}$ is readily solved for.

This conditional entropy is bound below by zero and above by $\log(k^4)$. Zero is achieved when, for all $\hat{P}_i^{[n]} > 0$, $\hat{P}_{is}^{[n,n+1]} = 1$ for some particular s (that may depend on i) and $\hat{P}_{is'}^{[n,n+1]} = 0$ for all $s \neq s'$. The $\log(k^4)$ is achieved when, for all $\hat{P}_i^{[n]} > 0$, the $\hat{P}_{is}^{[n,n+1]}$ are equal for all s and therefore equal $1/k^4$. In other words, the lower bound is achieved when each parent pixel can only be subdivided into child pixels of one category, and the upper bound is achieved when there is an even distribution of categories among child 4-tuples that are nested within parent pixels of a common parent category.

To use the terminology of Colwell (1974), the upper bound implies a state of maximum conditional entropy and zero predictability of the $n+1$ scale map, given the n scale map, while the lower bound implies zero conditional entropy and complete predictability of the $n+1$ scale map, given the n scale map. For actual landscapes, it is unlikely to ever see a maximum conditional entropy of $\log(k^4)$, but rather a lower maximum that is a function of the marginal land cover distribution.

When conditional entropy is plotted as a function of increasing pixel size (decreasing resolution), we trace a *conditional entropy profile*, examples of which appear in following chapters. This simple 2-dimensional plot reflects characteristics of both the marginal land cover distribution and multi-scale spatial pattern.

2.1 Computing Conditional Entropy of Expected Frequencies based on Single -Resolution Maps

Multi-resolution data for the framework that was just described is seldom available in practice. More typically, only a single resolution

map is available, referred to as the “floor” resolution. We may obtain a sequence of increasingly coarser maps from this floor resolution map, by successive application of a resampling filter, whereby parent pixels are assigned categories according to some function of its corresponding children pixels.

Several approaches to resampling are available. For example, Costanza and Maxwell (1994) chose the northwest corner child pixel to assign its category to the respective parent pixel. A modal filter (i.e. Benson and Mackenzie, 1995) may also be used, which has intuitive appeal; however, the child pixels can easily not always yield a single mode; therefore, “ties” need to be broken at random anyhow. A modal filter is more appealing for larger resampling windows, such as when aggregating 3x3 or more child pixels into each parent.

A random filter, which chooses one of the child pixels with equal probability, is a close approximation to the modal filter. Most importantly, the random filter allows for computation of expected frequencies $P_i^{[n]} = E[\hat{P}_i^{[n]}]$, $P_s^{[n+1]} = E[\hat{P}_s^{[n+1]}]$ and $P_{s,i}^{[n+1,n]} = E[\hat{P}_{s,i}^{[n+1,n]}]$, as discussed shortly. We can therefore obtain the entropy of these expected frequencies, which is much more meaningful than calculating conditional entropy for one particular simulation of the random filter. Even if we simulated the random filter many times, calculating the conditional entropy for each replication and taking the average, such a sample entropy is well known to be biased (i.e. Basharin, 1959). For these reasons, we chose to work with a random filter so we could obtain the expected frequencies and subsequent entropies, as discussed next. Further computational details and supporting theory are found in Johnson, Myers, Patil and Taillie (1998) and Johnson, Myers, Patil and Taillie (2001a).

By virtue of the random filter, the category (or color) of each pixel at each resolution is a random variable, so we must consider corresponding “color” distributions. For example, a pixel u in map M_n has a color distribution such that $f_u^{[n]}(i)$, for $i = 1, \dots, k$, is the probability that pixel u is assigned color i . Letting (v_1, v_2, v_3, v_4) be the 4-tuple of child pixels of u in map M_{n+1} , the random filter implies that

$$f_u^{[n]}(i) = \frac{1}{4}(f_{v_1}^{[n+1]}(i) + f_{v_2}^{[n+1]}(i) + f_{v_3}^{[n+1]}(i) + f_{v_4}^{[n+1]}(i)). \quad (2.6)$$

In other words, when using the random filter, the probability of assigning the i^{th} color to pixel u in map M_n equals the average probability that the i^{th} color is assigned to each child pixel in map M_{n+1} that is nested within pixel u . Therefore, instead of actually applying the random filter to map M_{n+1} to obtain one particular realization of map M_n , an overall distribution of possible colors can be obtained by the *linear filter* on

spatially referenced color distributions that is presented by Equation 2.6.

The “floor” resolution map (M_L), which was obtained directly from the data, has a degenerate color distribution for each pixel because the colors are known. In other words, at the floor resolution, $f_v^{[L]}(i) = 1$ if pixel v has color i and $f_v^{[L]}(i) = 0$ otherwise. Starting with the floor resolution, the color distributions at successively coarser resolutions are obtained by recursively applying Equation 2.6.

If we let $\mathbf{s}=(j_1, j_2, j_3, j_4)$ be a 4-tuple of colors, then the probability that the colors \mathbf{s} are assigned to the 4-tuple of pixels $\mathbf{v}=(v_1, v_2, v_3, v_4)$ is

$$f_{\mathbf{v}}^{[n+1]} \equiv f_{v_1}^{[n+1]}(j_1)f_{v_2}^{[n+1]}(j_2)f_{v_3}^{[n+1]}(j_3)f_{v_4}^{[n+1]}(j_4). \quad (2.7)$$

While equation 2.7 is not true for random maps in general, it is obviously true for the deterministic floor resolution map and holds true for the successively coarser resolution maps because they are obtained by applying the random filter independently in each 2×2 window.

Now we can obtain the expected marginal distribution of 4-tuple colors for the $n + 1$ resolution, $P_{\mathbf{s}}^{[n+1]}$, for $\mathbf{s} = 1, \dots, k^4$, by averaging the expression in Equation 2.7 over N_n windows \mathbf{v} in map M_{n+1} , such as

$$P_{\mathbf{s}}^{[n+1]} = \frac{1}{N_n} \sum_{\mathbf{v}} f_{v_1}^{[n+1]}(j_1)f_{v_2}^{[n+1]}(j_2)f_{v_3}^{[n+1]}(j_3)f_{v_4}^{[n+1]}(j_4). \quad (2.8)$$

However, if masking of floor resolution pixels is necessary, we must delete 4-tuples \mathbf{s} containing “nodata” values and renormalize the $P_{\mathbf{s}}^{[n+1]}$ table. Note that N_n is the number of pixels in map M_n that also equals the number of 2×2 non-overlapping windows in map M_{n+1} .

Next we consider the marginal probabilities $P_i^{[n]}$. These probabilities do not depend upon the resolution n when the datamap is square of size $2^L \times 2^L$. If pixel-masking is necessary, then $P_i^{[n]}$ can vary slightly with the resolution n . First, observe that

$$P_i^{[n]} = \frac{1}{N_n} \sum_u f_u^{[n]}(i), \quad (2.9)$$

where N_n is the number of pixels in map M_n and the sum is over all pixels u in map M_n . Again, deletion of the “nodata” value i and renormalization of the table is required in case of pixel-masking. Summing both sides of equation 2.6 with respect to u and using the fact that $4N_n = N_{n+1}$ establishes the earlier claim that $P_i^{[n]}$ does not depend upon n when there is no pixel-masking. The argument breaks down when there is pixel-masking because the sum must exclude the “nodata” values.

Table 2.2. The five types of 4-tuples \mathbf{s} and corresponding values of $Q_{\mathbf{s}}$ in equation 2.11, using natural logarithms. The second column gives a canonical permutation of the components of \mathbf{s} and the third column is obtained from equation 2.10.

Type	$j_1 j_2 j_3 j_4$	$P_{\mathbf{s},i}^{[n+1,n]}$	$Q_{\mathbf{s}}$
1	AAAA	δ_{Ai}	$-1 \log 1 = 0$
2a	AAAB	$\frac{3}{4}\delta_{Ai} + \frac{1}{4}\delta_{Bi}$	$-\frac{3}{4} \log \frac{3}{4} - \frac{1}{4} \log \frac{1}{4} = 0.562$
2b	AABB	$\frac{1}{2}\delta_{Ai} + \frac{1}{2}\delta_{Bi}$	$-\frac{1}{2} \log \frac{1}{2} - \frac{1}{2} \log \frac{1}{2} = 0.693$
3	AABC	$\frac{1}{2}\delta_{Ai} + \frac{1}{4}\delta_{Bi} + \frac{1}{4}\delta_{Ci}$	$-\frac{1}{2} \log \frac{1}{2} - \frac{2}{4} \log \frac{1}{4} = 1.04$
4	ABCD	$\frac{1}{4}(\delta_{Ai} + \delta_{Bi} + \delta_{Ci} + \delta_{Di})$	$-\frac{4}{4} \log \frac{1}{4} = 1.386$

Meanwhile, the conditional probability distribution of colors in map M_n , given the respective 4-tuples of colors in M_{n+1} , is readily obtained by the following relationship. For color vector $\mathbf{s}=(j_1, j_2, j_3, j_4)$,

$$P_{\mathbf{s},i}^{[n+1,n]} = \frac{1}{4}(\delta_{j_1,i} + \delta_{j_2,i} + \delta_{j_3,i} + \delta_{j_4,i}), \quad (2.10)$$

where $\delta_{j,i}$ is the kronecker delta function such that

$$\delta_{j,i} = \begin{cases} 1 & \text{if } j = i \\ 0 & \text{otherwise.} \end{cases}$$

The formidable-looking expression,

$$Q_{\mathbf{s}} = - \sum_{i=1}^K P_{\mathbf{s},i}^{[n+1,n]} \log(P_{\mathbf{s},i}^{[n+1,n]}), \quad (2.11)$$

that appears in equation 2.3 is actually quite simple and does not depend on the resolution n or on the floor resolution map. We are going to show that $Q_{\mathbf{s}}$ takes on only five distinct values as \mathbf{s} ranges over the K^4 different 4-tuples.

First observe, from equation (2.10), that $Q_{\mathbf{s}}$ is unchanged when the components of $\mathbf{s} = (j_1, j_2, j_3, j_4)$ are permuted. The 4-tuples \mathbf{s} can be classified into four different types depending on the number of distinct colors among j_1, j_2, j_3, j_4 . The 4-tuples of type 2 (i.e., those with exactly two distinct colors) can be further classified into two subtypes depending on whether the two colors are distributed among the four pixels in a 50-50 split or a $\frac{1}{4}$ - $\frac{3}{4}$ split. Table 2.2 lists the five different types of 4-tuples \mathbf{s} and the corresponding values of $Q_{\mathbf{s}}$ for a natural logarithm. The second column of the table gives a canonical permutation of the components of \mathbf{s} for each type.

Equation 2.3 now takes the simple form of a linear combination of the probabilities (with respect to the random filter) of occurrence of the different types of 4-tuples in M_{n+1} :

$$\begin{aligned}
 H^{[n,n+1]} &= \sum_{\mathbf{s}} P_{\mathbf{s}}^{[n+1]} Q_{\mathbf{s}} \\
 &= 0.562 \sum_{\mathbf{s}:type2a} P_{\mathbf{s}}^{[n+1]} + 0.693 \sum_{\mathbf{s}:type2b} P_{\mathbf{s}}^{[n+1]} \\
 &\quad + 1.04 \sum_{\mathbf{s}:type3} P_{\mathbf{s}}^{[n+1]} + 1.386 \sum_{\mathbf{s}:type4} P_{\mathbf{s}}^{[n+1]}. \quad (2.12)
 \end{aligned}$$

One now has all of the “ingredients” for obtaining the marginal and conditional entropies of the probability distributions $P_i^{[n]}$, $P_{\mathbf{s}}^{[n+1]}$ and $P_{\mathbf{s},i}^{[n+1,n]}$, which are $H^{[n]}$, $H^{[n+1]}$ and $H^{[n+1,n]}$, respectively. Therefore, Equation 2.5 can now be used to obtain the conditional entropy of the probability of going to a child 4-tuple of colors \mathbf{s} at scale $n+1$, given the parent color i at scale n , such that

$$\begin{aligned}
 H^{[n,n+1]} &= - \sum_{i=1}^k P_i^{[n]} \sum_{\mathbf{s}=1}^{k^4} P_{i\mathbf{s}}^{[n,n+1]} \log P_{i\mathbf{s}}^{[n,n+1]} \\
 &= H^{[n+1]} + H^{[n+1,n]} - H^{[n]}. \quad (2.13)
 \end{aligned}$$

We then obtain an explicit expression for conditional entropy by substituting the terms $P_i^{[n]}$ and $P_{\mathbf{s}}^{[n+1]}$ into equations 2.1 and 2.2, respectively, then combining with equations 2.12 and 2.13, resulting in

$$\begin{aligned}
 H^{[n,n+1]} &= - \sum_{\mathbf{s}} P_{\mathbf{s}}^{[n+1]} \log(P_{\mathbf{s}}^{[n+1]}) + \sum_{i=1}^K P_i^{[n]} \log(P_i^{[n]}) \\
 &\quad + 0.562 \sum_{\mathbf{s}:type2a} P_{\mathbf{s}}^{[n+1]} + \sum_{\mathbf{s}:type2b} P_{\mathbf{s}}^{[n+1]} \\
 &\quad + 1.04 \sum_{\mathbf{s}:type3} P_{\mathbf{s}}^{[n+1]} + 1.386 \sum_{\mathbf{s}:type4} P_{\mathbf{s}}^{[n+1]}. \quad (2.14)
 \end{aligned}$$

Landscape Pattern Analysis for Assessing Ecosystem
Condition

Johnson, G.D.; Patil, G.P.

2007, XVIII, 130 p. 73 illus., 2 illus. in color., Hardcover

ISBN: 978-0-387-37684-4